Time-Resolved CIDNP Study of Native-State Bovine and Human α-Lactalbumins

Olga B. Morozova,[†] Alexandra V. Yurkovskaya,*[,†] Renad Z. Sagdeev,[†] K. Hun Mok,[‡] and P. J. Hore[§]

International Tomography Center of SB RAS, 630090, Institutskaya 3a, Novosibirsk, Russia, Oxford Centre for Molecular Sciences, Oxford University, Central Chemistry Laboratory, South Parks Road, Oxford, OX1 3QH, United Kingdom, and Physical and Theoretical Chemistry Laboratory, Oxford University, South Parks Road, Oxford, OX1 3QZ, United Kingdom

Received: February 11, 2004; In Final Form: June 18, 2004

The reaction mechanism and details of the formation of CIDNP (chemically induced dynamic nuclear polarization) in the photoreactions of two aromatic dyes (2,2′-dipyridyl, DP, and flavin mononucleotide, FMN) with bovine and human α-lactalbumins (BLA and HLA) in aqueous solution have been studied using the time-resolved CIDNP technique. With DP as the photosensitizer, polarization in BLA is observed for the protons of Trp118, His68, Tyr18, and Tyr103. The latter is not manifested in the CIDNP spectra obtained with FMN. This threshold effect on CIDNP formation indicates that accessibility is a combined property of both the residue and the dye. The nuclear spin−lattice relaxation times in the radicals formed in these reactions have been determined from the CIDNP kinetics: $T_1 = 60$ μs for H2,4,7 of Trp118, $T_1 = 53$ μs for H3,5 of Tyr103, $T_1 = 16$ μs for H3,5 of Tyr18, and $T_1 = 10$ μs for the H2 and H4 of His68. The correlation times for the side chain motion as determined from the T_1 of the radicals are correlated with the accessibility of the side chains in the intact protein.

Introduction

As a technique for studying biological macromolecules, NMR spectroscopy is not only capable of determining three-dimensional structures at atomic resolution but can also be used to investigate time-dependent behavior, including intramolecular dynamics and reaction kinetics. Historically, NMR spectroscopy of macromolecules was limited by its low inherent sensitivity and by the complexity of the spectra.[1] A method of increasing the sensitivity uses the phenomenon of chemically induced dynamic nuclear polarization (CIDNP). Nonequilibrium nuclear magnetization arises from the ability of magnetic nuclei to alter the electronic spin state of a transient radical pair and so to modulate its reactivity, resulting in anomalous NMR intensities for the nuclei involved. The observed polarization is determined by the magnetic resonance parameters of the transient radicals (*g*-factors and hyperfine constants) and by the multiplicity of the radical pair precursor (for reviews see two monographs[2,3] and two major reviews[4,5]).

In 1978, Kaptein demonstrated that CIDNP generated in photochemical reactions between an excited dye and certain amino acid side chains on the surface of a protein could be used to monitor the solvent accessibility or exposure of these residues.[6,7] As well as the strong enhancement of the NMR signals, CIDNP has the important feature that of the twenty common amino acids, usually only tyrosine, tryptophan, and histidine are potentially reactive with a photoexcited dye via electron or hydrogen atom transfer.[5,8] As a result, the CIDNP spectrum of a protein usually contains only a small subset of the many lines that constitute the conventional NMR spectrum. This "photo-CIDNP" technique has proven to be a useful probe of protein structure and of the wide variety of factors that modify the accessibility of the polarizable amino acid residues[5,9] including the structural changes that occur during protein folding.[5,10−14]

Hitherto, the overwhelming majority of protein CIDNP experiments have been performed using essentially continuous illumination, under steady-state conditions.[4−7,9−14] The signal intensity detected in such experiments depends on many factors such as spin dynamics, nuclear paramagnetic relaxation in the radicals, and the kinetics of the radical reactions so that only a qualitative interpretation is possible in many cases. An alternative approach is a time-resolved (TR) version of the technique, which allows high-resolution CIDNP spectra to be detected on a microsecond (or even sub-microsecond) time scale using nanosecond laser pulses to initiate the radical reactions.[15,16] In an ongoing project using TR-CIDNP, we have explored systematically the mechanism and details of CIDNP formation in the three amino acids, tryptophan, tyrosine, and histidine[17−19] and in small peptides containing one or more of these residues in aqueous solution.[20,21] Quantitative analysis of the CIDNP kinetics of the amino acids provided information about nuclear paramagnetic relaxation and the rate constants of degenerate electron exchange between the amino acid radicals and their parent diamagnetic molecules. Armed with these data, we performed the first TR-CIDNP study of a small protein—a hen egg-white lysozyme in its native and denatured states.[22] The results showed that CIDNP in proteins depends not only on the accessibility of the amino acid residues and on the mechanisms of their photochemical reactions[8,17−19] but also on the dynamic properties of the intermediate radicals, on their nuclear paramagnetic relaxation, and on the efficiency of intramolecular electron-transfer reactions in the protein.[22]

The present paper describes a time-resolved CIDNP study of bovine and human *holo* α-lactalbumins (BLA and HLA,

* Author for correspondence. Tel.: +7 3832 331333; fax: +7 3832 331399; e-mail: yurk@tomo.nsc.ru.
[†] International Tomography Center of SB RAS.
[‡] Oxford Centre for Molecular Sciences.
[§] Physical and Theoretical Chemistry Laboratory.

10.1021/jp049385o CCC: $27.50
Published on Web 08/28/2004

TABLE 1: Total Side Chain Accessibilities (TSA) of the Potentially CIDNP Active Residues in the Native States of BLA[27] and HLA[28]

	TSA for BLA (HLA), %[a]		
	probe size, Å		
residue number	1.4	3.0	5.0
Trp26 (Leu26)	0.1 (n.a.[b])	0.0 (n.a.)	0.0 (n.a.)
Trp60	2.1 (3.8)	0.0 (0.0)	0.0 (0.0)
Trp104	3.6 (3.8)	0.0 (0.0)	0.0 (0.0)
Trp118	13.5 (10.0)	1.75 (0.25)	0.03 (0.0)
Tyr18	38.5 (39.3)	21.5 (24.5)	11.9 (16.7)
Tyr36	9.3 (8.4)	1.68 (0.72)	0.01 (0.0)
Tyr50	10.8 (13.9)	1.2 (4.62)	0.0 (0.11)
Tyr103	19.4 (12.6)	2.52 (2.22)	0.11 (0.0)
His32	34.4 (32.8)	17.9 (15.5)	8.32 (6.50)
His68 (Gln68)	97.5 (n.a.)	75.1 (n.a.)	58.6 (n.a.)
His107	10.7 (6.2)	3.09 (0.52)	0.74 (0.0)

[a] Total side chain accessibilities (TSA) refer to the percentage of accessible surface area for the entire side chain of the residue relative to the surface accessibility of the same residue type in an Ala-X-Ala tripeptide. [b] Not applicable as the amino acid residue type in HLA is different from that of BLA and hence not polarizable with CIDNP.

respectively). These small monomeric globular proteins both contain 123 residues and show close homology to hen lysozyme. In their native states, α-lactalbumins and lysozyme have similar conformations but are quite different in two respects: in their ability to bind Ca^{2+} ions and in their folding properties.[23] The first steady-state CIDNP study of various α-lactalbumins, including BLA and HLA, was performed by Berliner and Kaptein in 1981.[24] It was found that His68, Trp118, Tyr18, and Tyr 103 are the only polarizable residues among the three histidine, four tryptophan, and four tyrosine residues in BLA, and for each amino acid type only the most accessible residue was polarized. This led to the conclusion that the signal intensity correlates *qualitatively* with solvent accessibility.[24] This correlation is illustrated by the data in Table 1 and will be discussed below. Here, we concentrate on the methodology of TR-CIDNP as applied to proteins to demonstrate the type of site-specific information on dynamic properties that can be gleaned from an analysis of CIDNP spectra and kinetics. The main goal is to establish the *quantitative* relationship between the intensities in the CIDNP spectrum and such parameters as the accessibility, reactivity, and intramolecular mobility of the polarizable amino acid side chains. We compare CIDNP data for BLA and HLA using two dyes as photosensitizers: 2,2′-dipyridyl (DP), which efficiently generates CIDNP in amino acids using UV light from a pulsed excimer laser,[17−22] and flavin mononucleotide (FMN), which has been widely used in steady-state experiments.[4−15,24,25] Here, we demonstrate that the geminate CIDNP enhancements provide a more reliable surface probe than do the steady-state signals and that the former are determined not only by the accessibility of an amino acid residue but also by the size of the sensitizer and the rate of the reaction of the triplet dye with the residue. Simulation of the experimental CIDNP kinetic data provides the rates of nuclear paramagnetic relaxation of individual protons in the radicals derived from the (partially) accessible residues, giving the opportunity to extract valuable site-specific information about intramolecular mobility.

Experimental Section

The samples, sealed in a standard 5-mm NMR Pyrex ampule, were irradiated by a COMPEX Lambda Physik excimer laser (wavelength 308 nm, pulse energy up to 150 mJ) in the probe of a 200 MHz Bruker DPX-200 NMR spectrometer. Light was guided to the sample using an optical system containing a quartz lens, a prism, and a cylindrical light guide (5-mm diameter), which was placed off-center inside the Bruker NMR probehead. The upper end of the light guide was cleaved at 45° to direct the light horizontally through the saddle coil into the sample. Photometric measurements showed that 20−25% of the light from the laser reaches the sample. TR-CIDNP experiments were carried out with the usual pulse sequence: radio frequency (RF) saturation pulses−laser pulse−evolution time τ−RF detection pulse−free induction decay. WALTZ16 was used for the presaturation. As the background signals in the spectrum originating from equilibrium polarization are suppressed, only resonances from the polarized products formed during the variable delay τ appear in the CIDNP spectra. In all kinetic measurements, an RF pulse with a duration of 4 μs was used. The times plotted in Figures 6−8 correspond to the interval between the light flash and the center of the RF pulse (e.g., 2 μs for $\tau = 0$) on all plots in Figures 6−8. The synchronization of the laser pulse and the detection pulse was provided by a digital delay generator (Stanford Research System DG535), controlled by an oscilloscope using an RF-induced signal from a pickup antenna inserted next to the NMR coil and a signal from a fast photodiode placed in the laser beam.

Each of the four sets of kinetic data (BLA + FMN, BLA + DP, HLA + FMN, HLA + DP) was recorded using 16 samples: each sample was used to acquire 4 scans for each of 10 τ-values, so that every data point in Figures 6−8 represents 64 signal accumulations. The sample depletion after the 40 light flashes was never more than 20%. To avoid any distortion of the kinetics from this source, ascending and descending orders of the time delays were used alternately.

D_2O (Aldrich), BLA (Sigma), DP (Aldrich), *N*-acetyl tryptophan (Aldrich), *N*-acetyl tyrosine (Aldrich), *N*-acetyl histidine (Aldrich), FMN (Sigma), and sodium cacodylate (Aldrich) were used as received. The HLA sample was a generous gift from Prof. Valentina Bychkova (Institute of Protein Research of the Russian Academy of Sciences, Pushchino, Moscow region, Russia). Concentrations were 1.5 mM for the proteins, 14 mM for DP, and 2.5 mM for FMN. The pH was adjusted by addition of DCl or NaOD. No correction was made for the deuterium isotope effect on the pH. The relative intensities of signals in the CIDNP spectra did not depend on the FMN or DP concentrations.

Static solvent accessibility calculations were performed using Naccess version 2.1.1[26] on the X-ray crystallographic structures of native BLA and HLA (Protein Data Bank accession numbers 1F6S[27] and 1HML,[28] respectively). The program calculates the accessible surface area using the method of Lee and Richards[29] by rolling a sphere of specified size on the van der Waals surface of the protein. Probe sizes were varied from 0.3 to 1.4 Å (which is the default value representing the radius of a water molecule for the calculation of the Connolly surface), continuing up to 16.0 Å, and the relative surface accessibility values were compared. When using probes other than 1.4 Å, the total side chain surface accessibilities of the free amino acids were reevaluated and adjusted before utilization as the fully solvent accessible reference set.

Results and Discussion

A. Geminate CIDNP Analysis. Bovine and human α-lactalbumins have two subdomains: the α-domain comprises four

TABLE 2: Mechanisms of the Reaction of Triplet Dyes with *N*-Acetyl Derivatives of Tryptophan, Tyrosine, and Histidine and Values of the Corresponding Quenching Rate Constants

quenching reaction	quenching rate constant[a]/$M^{-1}s^{-1}$	reaction mechanism
$^{T}DP + TrpH \rightarrow DP^{-\bullet} + TrpH^{+\bullet}$	4.0×10^9 (ref 17)	e^- transfer
$^{T}DP + TyrOH \rightarrow DPH^{\bullet} + TyrO^{\bullet}$	2.2×10^8 (ref 19)	H transfer
$^{T}DP + HisH_2^{+} \rightarrow DPH^{\bullet} + HisH^{+\bullet}$	2.8×10^7 (ref 18)	H transfer
$^{T}FMN + TrpH \rightarrow FMN^{-\bullet} + TrpH^{+\bullet}$	2.3×10^9 (ref 31)	e^- transfer
$^{T}FMN + TyrOH \rightarrow FMN^{-\bullet} + TyrOH^{+\bullet}$	1.5×10^9 (ref 31)	e^- transfer
$^{T}FMN + HisH \rightarrow FMNH^{\bullet} + His^{\bullet}$	2.0×10^8 (ref 31)	H transfer

[a] Recorded at pH 6.5 for DP and pH 7.7 for FMN.

α-helices and one small region of 3_{10}-helix near the C-terminus; the remainder of the protein (residues 40−81) constitutes the *β*-domain, containing three short *β*-strands. Figure 1 shows the

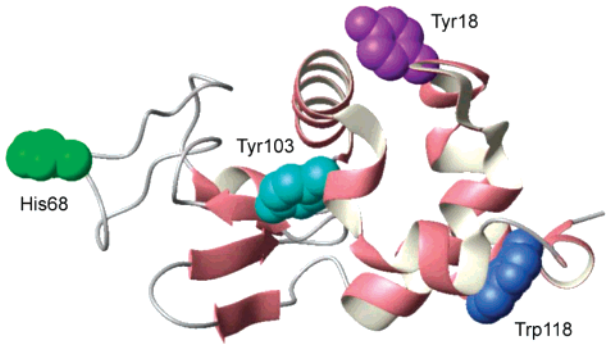

Figure 1. Ribbon representation of the three-dimensional structure of bovine α-lactalbumin. The side chains of CIDNP-active residues are shown. The diagram was generated using the PDB coordinates for BLA (1F6S)[27] using the program MOLMOL 2K.1.[30]

structure of the bovine protein with the locations of the CIDNP-active residues Trp118, Tyr18, Tyr103, and His68 indicated.

Side Chain Accessibilities. The calculated total side chain accessibilities (TSA) of the tryptophan, tyrosine, and histidine residues in BLA are collected in Table 1.

Mechanisms and Rates of Reactions. In earlier publications, we have reported in detail on the mechanisms of the reactions between triplet excited dyes and *N*-acetyl derivatives of the amino acids.[17−19,31] Quenching rate constants have been measured using laser flash photolysis and the reaction mechanisms have been established over a wide pH range. The results for neutral pH are summarized in Table 2.

The triplet states of the two dyes are characterized by the ionization constants $pK_a = 5.8$ for $^{T}DPH^{+}$[17] and $pK_a = 4.4$ for $^{T}FMNH^{+}$;[31−33] in neutral solution they both exist in the deprotonated, neutral form. Reaction with tryptophan proceeds via electron transfer for both dyes.[8,17,31]

Tyrosine also reacts with ^{T}FMN by electron transfer,[19] although the quenching mechanism was originally thought to be hydrogen atom transfer at neutral pH.[8] The mechanism of the reaction of ^{T}DP and tyrosine is hydrogen atom transfer with a quenching rate constant approximately an order of magnitude lower than typical electron-transfer rates for amino acids.[19] Direct use of these rate constants for the free amino acids to estimate the reactivity of the corresponding residues in a protein is not always possible, since the reactivity of a free amino acid and of a fully accessible amino acid residue in a polypeptide chain may differ significantly. Our previous comparative study of geminate CIDNP in binary mixtures of tryptophan and tyrosine and in the dipeptide Trp-Tyr revealed an increase in the reactivity of the tyrosine side chain toward ^{T}DP in neutral solution upon incorporation into the dipeptide,[21] while the accessibility stays approximately the same.

Turning to histidine, the mechanism of the reactions with both ^{T}DP and ^{T}FMN is hydrogen atom transfer,[31] but different protonation states of the histidine are involved in the two cases: ^{T}DP reacts with histidine protonated on the imidazole ring,[18] $HisH_2^{+}$ ($pK_a = 6.1$),[34] while ^{T}FMN reacts with the neutral form HisH.[31] The maximum quenching rates occur at pH 6 for DP[18] and at pH 8 for FMN.[31] Our measurements of geminate CIDNP formed in the reaction of BLA with DP and with FMN show that the relative CIDNP enhancement of His68 has a pronounced pH dependence (not shown) which qualitatively correlates with the titration curve for the quenching rate constants for the *N*-acetyl histidine + dye reactions.[18,31] The value of $pK_a = 6.49$ for the solvent-exposed His68 in BLA[35] is higher than that of the free amino acid (6.1). Therefore, for our kinetic measurements, we have chosen pH 6.5 for the photoreaction with DP and pH 7.7 for the reaction with FMN to obtain the best signal-to-noise ratio in each case.

CIDNP Spectra. Figure 2 shows the aromatic region of the ^{1}H CIDNP spectra of BLA with FMN (left) and DP (right).

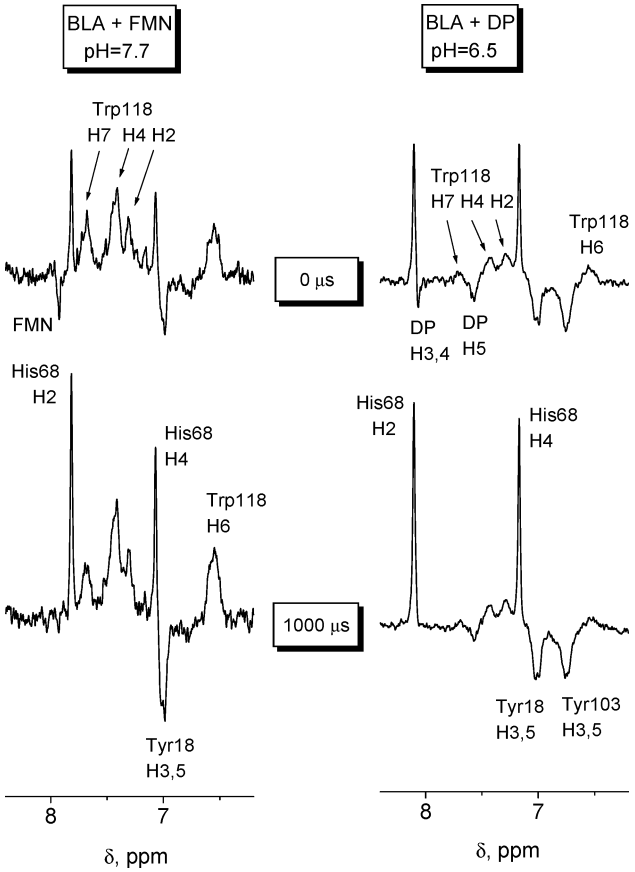

Figure 2. Aromatic region of the ^{1}H CIDNP spectra, obtained for native bovine α-lactalbumin with flavin mononucleotide at pH 7.7 in the presence of 50 mM sodium cacodylate (left), and with 2,2′-dipyridyl at pH 6.5 (right). The upper and lower spectra were recorded, respectively, immediately after and 1 ms after the laser pulse.

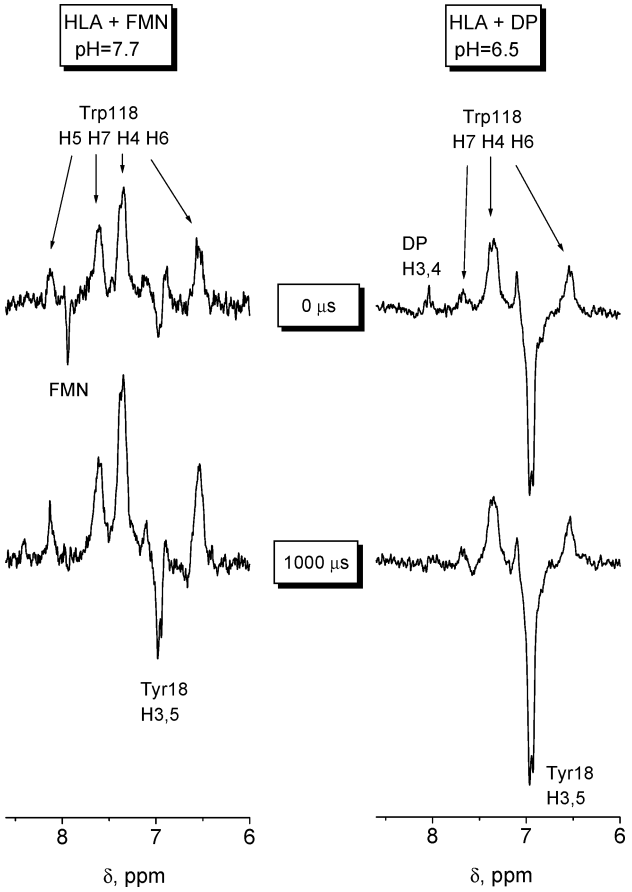

Figure 3. Aromatic region of the ^{1}H CIDNP spectra, obtained for native human α-lactalbumin with flavin mononucleotide at pH 7.7 in the presence of 50 mM sodium cacodylate (left), and with 2,2′-dipyridyl at pH 6.5 (right). The upper and lower spectra were recorded, respectively, immediately after and 1 ms after the laser pulse.

The upper pair of spectra were recorded immediately after the laser pulse ($\tau = 0$) and the lower pair at $\tau = 1$ ms. So, as to be able to compare our results with the steady-state CIDNP data,[12,13,25] the spectra of BLA with FMN were obtained under the same conditions as in refs 12 and 25, namely, in the presence of 50 mM of sodium cacodylate, which however did not affect either the kinetics or the amplitudes of the CIDNP signals. With DP, a strong attenuation in the CIDNP intensity was observed in the presence of sodium cacodylate, presumably caused by quenching of triplet DP by the buffer. Thus, measurements with DP were made without cacodylate. The pH of the unbuffered DP samples was not affected by sample illumination under the conditions of the CIDNP measurements. This was checked by direct measurement before and after irradiation and by noting that the pH-sensitive chemical shifts of the histidine resonances were not altered.

The spectrum of BLA with FMN at 1 ms (Figure 2, bottom left) is very similar to that recorded earlier using the steady-state CIDNP method.[4,12,14,25] Polarization is observed for H2 and H4 of His68; H2, H4, H6, and H7 of Trp118; and H3,5 of Tyr18. With DP as photosensitizer, signals of the same residues are detected, and additional polarization is observed for H3,5 of Tyr103, with intensity comparable to that of Tyr18. With FMN, a very weak signal is seen at the chemical shift of Tyr103. The ^{1}H NMR spectra of BLA are identical with and without DP and the chemical shifts of the DP protons are unaffected by the presence of the protein. It therefore seems unlikely that there is either significant protein−dye binding or dye-induced unfolding. CIDNP spectra of HLA are shown in Figure 3. Since this protein contains a glutamine instead of a histidine residue at position 68, only Trp118 and Tyr18 are polarized with both DP and FMN. In HLA, polarization of Tyr103 is observed only with DP. The lines of Tyr103 in HLA overlap with those of Tyr18, which gives rise to much more intense CIDNP; as a result, the signal from Tyr103 in HLA is not studied in the present work. The spectra obtained with FMN and DP show different relative enhancements for the various residues. For both proteins, the enhancements of Trp118 are lower relative to Tyr18 with DP than with FMN. A significant difference in the amplitudes of the His68 signals of BLA detected with no delay between the laser and RF pulses and with $\tau = 1$ ms is clearly seen in Figure 2: the H2 and H4 signals are twice as intense in the later spectra recorded with FMN but only 1.6 times with DP. For both proteins, the Tyr18 signal produced with FMN shows a pronounced growth as a function of time: the polarization is almost twice as strong at the longer delay, an increase that is noticeably smaller when DP is used as the dye.

In general, the spectra in Figures 2 and 3 suggest that the signal intensities observed in time-resolved spectra for long delays and in steady-state CIDNP spectra are only *qualitatively* correlated with amino acid side chain accessibility. For a more quantitative interpretation of CIDNP intensities in terms of side chain accessibility, it is necessary to consider time-resolved spectra recorded with no τ-delay in which, ideally, only *geminate* CIDNP is present, taking into account the reactivity and the CIDNP enhancement factors of the three amino acid types for the photosensitizer used. The latter are determined by the magnetic resonance parameters of the radicals and by the external magnetic field strength.

Side Chain Reactivities. In an attempt to estimate the reactivity of residues, we model the relative intensities of the geminate CIDNP in the spectra of BLA at $\tau = 0$ by measuring the geminate CIDNP in mixtures of three individual amino acids. Two mixtures of *N*-acetyl amino acids were studied: the first with equal concentrations (Figure 4, top) and the second with concentrations proportional to the reciprocal of the quenching rate constants (k_q) measured for the free amino acids (Figure 4, bottom) at the appropriate pH. The corresponding values of k_q are listed in Table 2. The second mixture is intended as a model of what would happen in the protein if all residues had the same reactivity and accessibility. Despite an almost 20-fold difference in quenching rate constants (Table 2), the CIDNP enhancements for tryptophan and tyrosine with DP in the equimolar mixture at pH 6.5 are comparable in size. Taking into account the deuterium isotope effect (0.4 unit difference between pH and pD) on both the measured pH values and the pK_a of ^{T}DP,[18] this is likely to be due to a strong contribution to the tyrosine enhancement from the much faster electron-transfer reaction with ^{T}DPH$^+$. Only at a pH almost two units higher than the pK_a of ^{T}DPH$^+$, (i.e., pH ∼ 8) is the CIDNP intensity of tyrosine significantly smaller than that of tryptophan in the equimolar mixture (Figure 5, right-hand side). Thus, in the spectrum that models the protein (Figure 4, lower right spectrum), the CIDNP intensity of tryptophan is lower than might otherwise be expected because of the larger rate constants for tyrosine and histidine residues compared to their values for the free amino acids, given in Table 2.

The rate constants for reaction of tyrosine and tryptophan with ^{T}FMN are only slightly dependent on pH.[31] The rate constant for the reaction histidine + ^{T}FMN has a flat maximum at pH ≈ 8, so the deuterium isotope effect does not have a

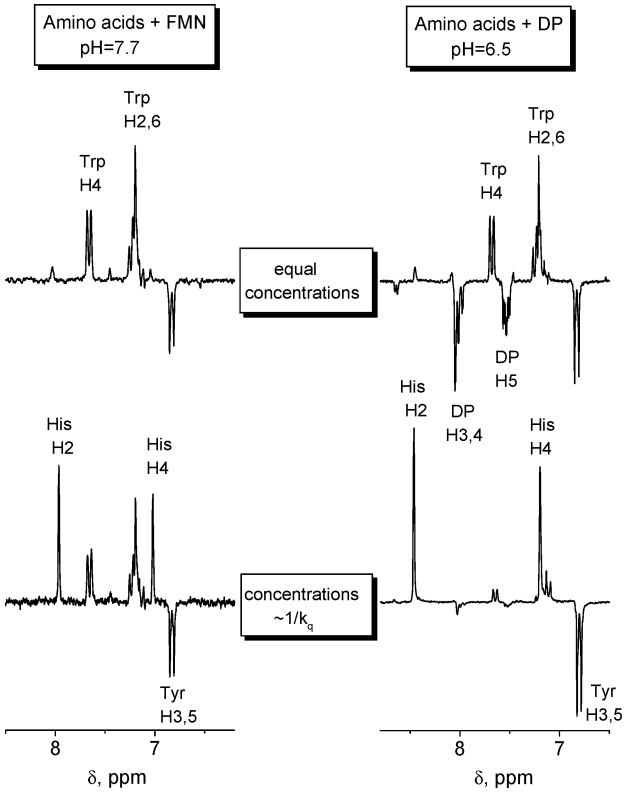

Figure 4. Aromatic region of the ^{1}H CIDNP spectra, obtained for mixtures of the *N*-acetyl derivatives of tryptophan, tyrosine, and histidine with flavin mononucleotide at pH 7.7 (left), and with 2,2′-dipyridyl at pH 6.5 (right) immediately after the laser pulse. Concentrations of the amino acids were 1.5 mM Trp, Tyr, and His (upper spectra); 0.5 mM Trp, 9 mM Tyr, 70 mM His (lower right spectrum); 1.5 mM Trp, 2.2 mM Tyr, 17 mM His (lower left spectrum).

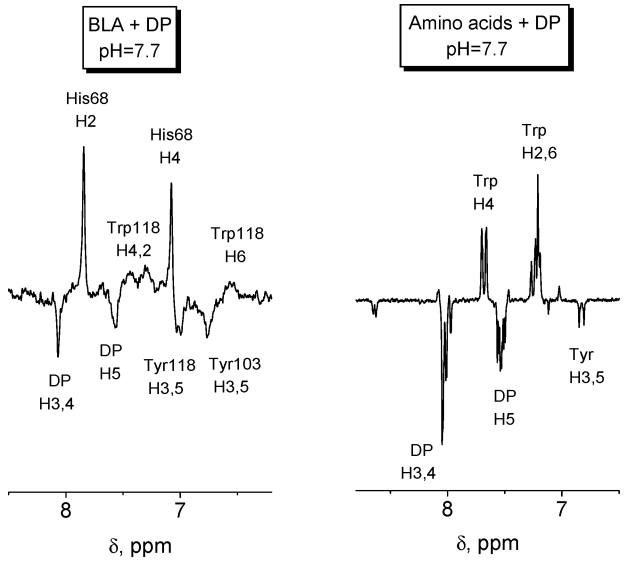

Figure 5. Aromatic region of the ^{1}H CIDNP spectra obtained for bovine α-lactalbumin (left) and an equimolar mixture (1.5 mM) of *N*-acetyl derivatives of tryptophan, tyrosine, and histidine (right) with 2,2′-dipyridyl at pH 7.7.

significant influence on k_q. This explains why the CIDNP spectrum of the amino acids with concentrations proportional to $1/k_q$ (Figure 4, bottom left) is very similar to the CIDNP spectrum of BLA with FMN recorded immediately after the laser pulse, indicating that the quenching rate constants for the polarizable residues in BLA are close to the values for the free amino acids.

The difficulties encountered in modeling DP-sensitized CIDNP intensities in proteins using the amino acid mixtures may be caused by the different reactivity of free and linked amino acids toward the triplet dye. This is illustrated in Figure 5, where DP-sensitized CIDNP spectra of BLA and an equimolar mixture of the amino acids at pH 7.7 are shown. By contrast to the free amino acids, the CIDNP spectrum of BLA contains signals of tryptophan and tyrosine of comparable intensities, although Tyr18 is more accessible on the protein surface than is Trp118. This leads us to the conclusion that reactivity of tyrosine toward the triplet DP is considerably increased in the protein. The increase of reactivity of tyrosine toward ^{T}DP has been earlier observed for the dipeptides Trp-Tyr,[21] where both residues are equally accessible.

Therefore, to extract reliable quantitative data about residue accessibility, one has to take into account the altered reactivity of the amino acids when they are incorporated into a peptide or protein and also measure the geminate CIDNP spectra. In addition, we would like to emphasize that accessibility is, strictly speaking, a combined property of both the residue and the dye. In our experiments, we do not observe a significant signal from Tyr103 using FMN, while this residue is strongly polarized by the smaller DP molecule. Tyr103 is located in the entrance of the active cleft of the protein (Figure 1) and its accessibility is determined by the width of the cleft and the size of the probing molecule. Apparently, DP can penetrate the cleft, while FMN cannot. Comparing the spectra using FMN and DP, similar threshold effects are not found for other residues although it would be reasonable to assume that their effective accessibility is somewhat smaller when FMN is used as the probe instead of DP. Table 1 contains the calculated TSAs for probes varying in radius from 1.4 to 5 Å. Earlier, Berliner and Kaptein[24] detected two CIDNP signals of tyrosine residues in the native state of BLA using the dye 3-*N*-carboxymethyl lumiflavin, which has almost the same size as FMN but no charged phosphate group. Thus, the threshold effect for Tyr103 may arise not only from the different sizes of DP and FMN but also from the ionic interaction of the phosphate group of FMN with the protein surface.

B. CIDNP Kinetics Analysis. Analysis of the CIDNP kinetics of radical reactions in solution can give valuable information about the structure of the radical intermediates, the kinetics of the creation of polarization in the diamagnetic reaction products, and the decay of nuclear polarization in the radicals via nuclear paramagnetic relaxation. The paramagnetic relaxation times are determined by the magnetic properties and intramolecular mobility of the amino acid residue radicals.

Kinetic CIDNP data for the polarizable residues in BLA and HLA are shown in Figures 6−8. All intensities were scaled in the same way, taking the signal of H2 of His68 at $\tau = 0$ as equal to 1. All resonances originating from the same residue (H2 and H4 of His68 and H2,4,7 and H6 of Trp118) showed similar behavior. Figure 6 shows the data for Tyr103 and Tyr18 (H3,5 protons). Figures 7and 8 contain, respectively, the data for the H2 resonance of His68 and for the overlapping H2,4,7 resonances of Trp118. For HLA, the resonances of Trp118 H2 and Tyr18 H3,5 overlap; therefore, only the experimental data for H4,7 of Trp118 in HLA (which are almost identical to the corresponding BLA data) are shown in Figure 8.

The details of the analysis of the CIDNP kinetics (originally suggested in ref 36) are presented in our earlier works[17−22] and

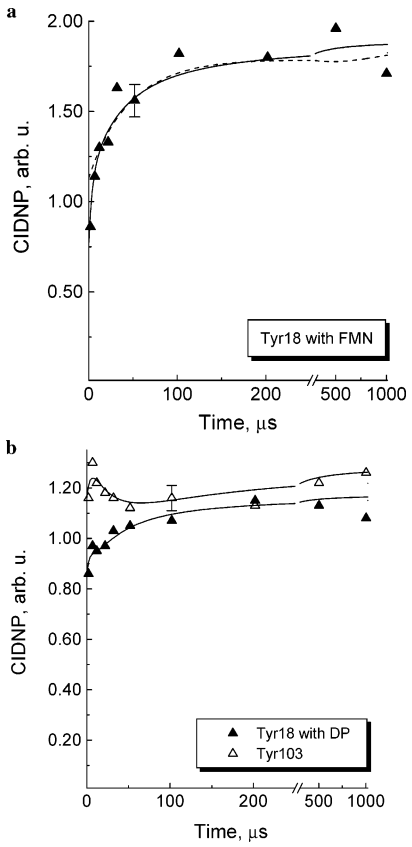

Figure 6. ^{1}H CIDNP kinetics, obtained for tyrosine residues of native bovine lactalbumin with flavin mononucleotide at pH 7.7 (a), and with 2,2′-dipyridyl at pH 6.5 (b): ▲, Tyr18; △, Tyr103. The lines were calculated according to the procedure described in the text. For the values of the parameters, see the text and Table 3.

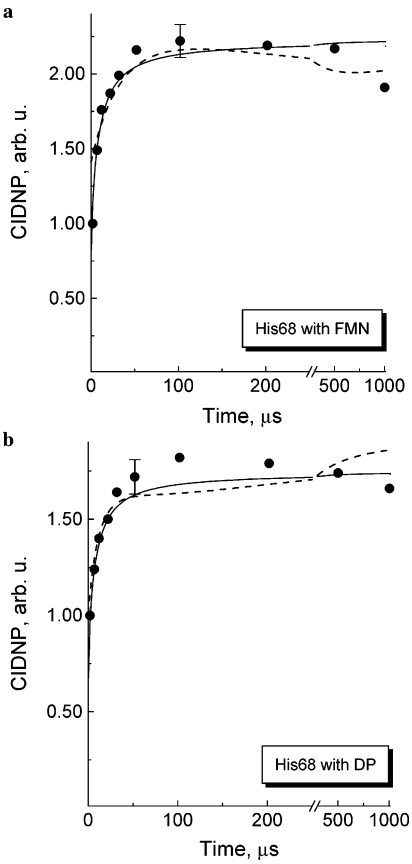

Figure 7. ^{1}H CIDNP kinetics, obtained for His68 of native bovine lactalbumin with flavin mononucleotide at pH 7.7 (a), and with 2,2′-dipyridyl at pH 6.5 (b). The lines were calculated according to the procedure described in the text. For the values of the parameters, see the text and Table 3.

are only briefly repeated here. CIDNP kinetics in the systems under study can be described by a set of differential equations:

$$R(t) = \frac{R_0}{1 + k_t R_0 t} \tag{1}$$

$$\frac{dP(R)}{dt} = -k_t P(R) R - k_t \beta R^2 - \frac{P(R)}{T_1} \tag{2}$$

$$\frac{dP(Pr)}{dt} = k_t P(R) R + k_t \beta R^2 \tag{3}$$

Here, R is the concentration of the radicals of interest, $P(R)$ and $P(Pr)$ are the polarizations of the radicals and the products, respectively, $R_0 k_t$ is the radical termination rate (where R_0 is the initial radical concentration and k_t is the termination rate constant), and T_1 is the nuclear paramagnetic relaxation time. The parameter β represents the polarization per radical pair, created in the radical pairs in the bulk, so-called F-pairs; it is related to the geminate polarization P^G via the quantity γ, which is the ratio of polarizations created in F- and geminate pairs:

$$\beta = \gamma P^G / R_0 \tag{4}$$

For the triplet precursor, $\gamma = 3$. As a rule, we use the value 2.8 for this parameter as suggested by Fischer et al.[36] This is acceptable if the radical pairs that participate in the geminate reaction are the same as those involved in the bulk termination. If secondary reactions leading to modification of the radicals take place, the value of γ may change as a result of pair substitution effects.[37,38]

On the right side of eqs 2 and 3, the first terms describe the transfer of polarization from the radicals to the diamagnetic molecules in the termination reaction, while the second terms represent the formation of polarization in F-pairs. The third term in eq 2 corresponds to the loss of polarization in the radicals because of nuclear paramagnetic relaxation.

It was assumed that the yield of radicals that escape from the triplet geminate radical pair is much greater than the yield of geminate recombination and that the radical pair partners decay only by recombining with one another with rate constant k_t. The initial polarizations were taken as $P(Pr) = P^G = -P(R)$, which is consistent with the spin sorting nature of the $S-T_0$ radical pair mechanism.

In both BLA and HLA, two types of kinetics were found. The first is characterized by a monotonic growth in the signal to reach a constant level. This behavior was observed for Tyr18 in both proteins and for His68 in BLA (the histidine signals show a slight falloff at times longer than 200 μs). The second type of kinetics was observed for all the tryptophan signals and for Tyr103 in BLA. The CIDNP data for these residues have maxima at relatively short times: ~6 μs for tyrosine and ~25 μs for tryptophan. The presence of a maximum in the CIDNP intensity at short times (and a minimum at later times) significantly constrains the parameter values during the fitting procedure, so improving their reliability. We therefore started with Tyr103 in BLA.

The best fit for the Tyr103 CIDNP kinetics in the reaction with DP (Figure 6b, open triangles) was obtained with $T_1 = 53$

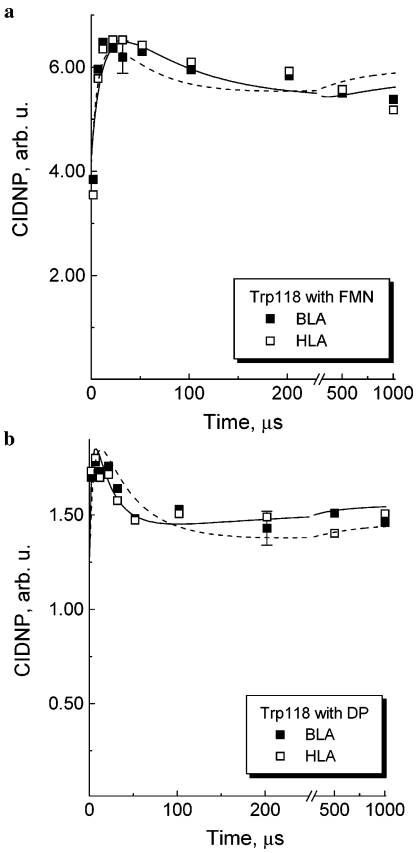

Figure 8. ^{1}H CIDNP kinetics, obtained for Trp118 of native bovine α-lactalbumin (■) and human α-lactalbumin (□) with flavin mononucleotide at pH 7.7 (a), and with 2,2′-dipyridyl at pH 6.5 (b). The lines were calculated according to the procedure described in the text. For the values of the parameters, see the text and Table 3.

μs and $R_0k_t = 6.9 \times 10^4$ s^{-1} (in this particular case only, $\gamma = 1.4$ was used instead of 2.8 as described in ref 19). It is reasonable to assume that the value of R_0k_t for Tyr18 with DP is twice that for Tyr103, because the former is about a factor of 2 more accessible. By fitting the data to the integrated rate equations for the CIDNP intensities, this allows us to determine that $T_1 = 16$ μs for Tyr18 (Figure 6b, filled triangles) and to use this value (which does not depend on the identity of the dye) to obtain $R_0k_t = 8.1 \times 10^4$ s^{-1} for the reaction of Tyr18 with FMN (Figure 6a, filled triangles).

For His68, the CIDNP signal grows rather rapidly to reach a stationary level about twice the initial polarization. Such behavior requires very efficient paramagnetic relaxation in the escaped radicals. Only with T_1 less than 10 μs could good agreement with the experimental data be obtained. Calculations for $T_1 = 10$ μs with $R_0\,k_t = 1.4 \times 10^5$ s^{-1} for FMN and $R_0k_t = 1.6 \times 10^5$ s^{-1} for DP are shown in Figure 7a and 7b, respectively. The fact that T_1 for the fully accessible His68 is considerably shorter than in the free amino acid (16 μs)[18] is in agreement with our finding that T_1 for dipeptides is about half the value for the free amino acids.[20,21] As was the case in our previous study of the free amino acids, histidine radicals have the shortest T_1 values, and the value of R_0k_t (which is similar to those obtained for tyrosine residues) is quite reasonable. In principle, satisfactory fits to the data can be obtained using a very long T_1 ($\approx$500 μs) and a rather small R_0k_t ($\approx 10^4$ s^{-1}) (dashed lines in Figures 6a and 7), but these values are highly unrealistic under the conditions of our experiments.

Fitting the Trp118 CIDNP kinetics (Figure 8) proved to be more complicated. We were unable satisfactorily to fit the kinetics obtained with the two sensitizers using a common value of T_1 and different R_0k_t (dashed lines in Figure 8, $T_1 = 125$ μs). Compared to the experimental data, the simulated kinetics evolve too slowly in DP ($R_0k_t = 8.0 \times 10^4$ s^{-1}) and too rapidly in FMN ($R_0k_t = 5.1 \times 10^4$ s^{-1}). This is surprising because T_1 is essentially a property of the radical derived from the amino acid residue and is not expected to depend on the identity of the dye. The best independent fits (solid lines in Figure 8) were obtained with the following parameters for Trp118: $R_0k_t = 3.3 \times 10^4$ s^{-1}, $T_1 = 220$ μs for FMN and $R_0k_t = 1.5 \times 10^4$ s^{-1}, $T_1 = 60$ μs for DP. The value of T_1 in FMN exceeds by a large margin those for the free amino acid (44 μs for H2,6 protons and 63 μs for the H4 proton in the tryptophan radical[17]). One possible reason for the discrepancy in T_1 for the two dyes could be binding of FMN to BLA in the vicinity of Trp118, arising from the Coulomb interaction between the anionic phosphate group of FMN and the cationic surface of the protein. This effect has been recently observed in the reaction of FMN with a hen egg-white lysozyme.[39]

The CIDNP kinetics for Trp118 in HLA are essentially identical to those for this residue in BLA (Figure 8, open squares). All values of the parameters T_1 and R_0k_t are listed in Table 3.

TABLE 3: Nuclear Paramagnetic Relaxation Times, Correlation Times, and Second-Order Termination Rate Constants for Bovine α-Lactalbumin

residue	T_1/μs	τ_e/ns	R_0k_t /s^{-1} (photosensitizer)	T_1/μs (protons in the radical of the corresponding free amino acid)
Trp118	220	26	3.3×10^4 (FMN)	44 (H2,6) ref 17
	60	6.9	1.5×10^5 (DP)	63 (H4) ref 17
Tyr103	53	5.2	no CIDNP (FMN)	63 (H3,5) ref 19
			6.9×10^4 (DP)	
Tyr18	16	0.8	8.1×10^4 (FMN)	
			1.2×10^5 (DP)	
His68	10	0.17	1.4×10^5 (FMN)	16 (H2, H4) ref 18
			1.6×10^5 (DP)	

C. Mobility of Amino Acid Residues. From the values of T_1 for different side chains, one can obtain estimates of the effective correlation times, τ_e, of their internal motion in the protein. We assume that the dependence of T_1 on τ_e is given by the simple relation

$$\frac{1}{T_1} = \frac{(\Delta B)^2 \tau_e}{1 + (\omega_N \tau_e)^2} \tag{5}$$

where ΔB is the strength of the local magnetic field whose stochastic modulation is responsible for the relaxation and ω_N ($=2\pi \times 200$ MHz) is the nuclear Larmor frequency. For the radicals derived from the free amino acids, the values of T_1(aa) are already known (see Table 3) and τ_e(aa) is assumed to be 100 ps. We further assume that ΔB is the same for the free amino acid and the corresponding residue in the protein. This allows us to determine τ_e(pr) for the side chain motion in the protein from the following relationship between T_1(aa) and T_1(pr):

$$\frac{T_1(\mathrm{pr})}{T_1(\mathrm{aa})} = \frac{\tau_e(\mathrm{aa})}{\tau_e(\mathrm{pr})} \times \frac{1 + (\omega_N \tau_e(\mathrm{pr}))^2}{1 + (\omega_N \tau_e(\mathrm{aa}))^2} \tag{6}$$

This quadratic expression for τ_e(pr) in general has two solutions. Values of τ_e(pr), obtained as described below, are presented in Table 3.

For Trp118 polarized using FMN, both roots of eq 6 for τ_e(pr) are physically meaningless: one is 24 ps (much shorter

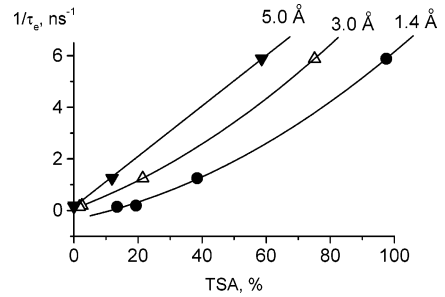

Figure 9. Dependence of the inverse correlation times of the internal motion of the CIDNP-active residues in BLA on their total side chain accessibility, calculated using different sizes of the probe (1.4, 3.0, 5.0 Å). Values of correlation times are given in Table 3.

than that for free tryptophan), the other is 26 ns (longer than the correlation time for the tumbling of the protein as a whole). However, the results for Trp118 polarized using DP are 90 ps and 6.9 ns. The former is shorter than that for the free amino acid radical and is discarded. The latter is apparently reasonable and can be used to characterize the mobility of the residue. A possible reason for the different behavior with the two dyes is, as discussed above, binding of FMN to the protein surface. For Tyr18, eq 6 gives two equal roots, $\tau_e(\mathrm{pr}) = 0.8$ ns, corresponding to the minimum in the plot of T_1 as a function of $\tau_e(\mathrm{pr})$. The two roots found for Tyr103 are $\tau_e(\mathrm{pr}) = 0.12$ ns and $\tau_e(\mathrm{pr}) = 5.2$ ns. The first is very close to the value (100 ps) used for the free amino acids and is too short to be realistic. The second (5.2 ns) seems physically reasonable.

For His68, the roots are $\tau_e(\mathrm{pr}) = 0.17$ ns and $\tau_e(\mathrm{pr}) = 3.8$ ns. Since His68 is almost completely exposed and therefore, presumably, very mobile, we choose the former.

It is reasonable to assume that the correlation times for the side chain motion as determined from the T_1 of the radicals are correlated with the accessibility of the side chains in the intact protein. If a residue is fully exposed to the sensitizer probe molecule, as appears to be the case for His68 (Figure 1), its motion is likely to be similar to that of the free amino acid. If, on the other hand, the amino acid residue is buried deep inside the protein, its motion will be significantly restricted and its correlation time is likely to be close to that for the protein as a whole (~10 ns).[40] As mentioned previously, the geminate CIDNP intensity depends on the accessibility, which is a combined property of the side chain and the probing dye molecule. However, in the absence of dye−protein association, relaxation times and mobilities should be probe-independent properties of the polarizable side chains. To see how the total side chain accessibility is related to the intramolecular mobility, we have calculated TSA values for the four polarized residues using different probe radii. The reciprocal of the correlation time, $1/\tau_e(\mathrm{pr})$, was a linear function of TSA for radii ≥ 5.0 Å (Figure 9); furthermore, the limiting value of $\tau_e(\mathrm{pr})$ (8.5 ns) for zero accessibility is close to the rotational correlation times determined for the native proteins from their hydrodynamic radii.[40] It therefore seems that the calculated side chain accessibility may be a good indicator of the intramolecular mobility.

Conclusion

A time-resolved CIDNP study of the reactions of two proteins, HLA and BLA, in their native state with two dyes (DP and FMN) has been carried out. It has been shown that the geminate CIDNP spectra (obtained with the shortest possible delay in a time-resolved measurement) can be used to analyze the accessibility and reactivity of amino acid residues toward the excited dye molecules. A comparative study of the CIDNP spectra of the proteins and mixtures of amino acids revealed an increased reactivity of tyrosine residues with triplet excited DP as compared to the free amino acids. The accessibility is a combined property of the residue and the photosensitizer, and a threshold effect has been observed for the accessibility of Tyr103 with different dyes.

From the analysis of the CIDNP kinetics, we obtained the nuclear spin−lattice relaxation times of radicals derived from the reactive residues and obtained qualitative information about the correlation times of their intramolecular motion. A decrease in the correlation time with increasing accessibility of the side chain has been observed.

A comparative study of CIDNP in the molten globule and denatured states of BLA is underway and will be described in a forthcoming paper.

Acknowledgment. We are grateful to Prof. V. Bychkova (Institute of Protein Research, Pushchino) for providing us with HLA. The financial support of RFBF (project No. 02-03-32765), INTAS (Project No. 02-2126), and the Russian Ministry of High Education (Grant 2298.2003.3) is gratefully acknowledged. A.V.Y. and O.B.M. are indebted to the Russian Science Support Foundation for financial support.

References and Notes

(1) Cavanagh, J.; Fairbrother, W. J.; Palmer, A. G.; Skelton, N. J. *Protein NMR spectroscopy: principles and practice*; Elsevier: San Diego, CA, 1996.

(2) *Chemically Induced Magnetic Polarization*; Muus, L. T., Atkins, P. W., McLauchlan, K. A., Pedersen, J. B., Eds.; D. Reidel: Dordrecht, The Netherlands, 1977.

(3) Salikhov, K. M.; Molin, Y. N.; Sagdeev, R. Z.; Buchachenko, A. L. *Spin Polarization and Magnetic Field Effects in Radical Reactions*; Molin, Yu. N., Ed.; Elsevier: Amsterdam, 1984.

(4) Kaptein, R. *Biol. Magn. Reson.* **1982**, *4*, 145−149.

(5) Hore, P. J.; Broadhurst, R. W. *Prog. Nucl. Magn. Reson. Spectrosc.* **1993**, *25*, 345−402.

(6) Kaptein, R.; Dijkstra, K.; Nicolay, K. *Nature* **1978**, *274*, 293−294.

(7) Kaptein, R. Structural information from photo-CIDNP in proteins. In *NMR Spectroscopy in Molecular Biology*; Pullman, B., Ed.; D. Reidel: Dordrecht, The Netherlands, 1978; pp 211−229.

(8) Stob, S.; Kaptein, R. *Photochem. Photobiol.* **1989**, *49*, 565−577.

(9) Broadhurst, R. W.; Dobson, C. M.; Hore, P. J.; Radford, S. E.; Rees, M. L. *Biochemistry* **1991**, *30*, 405−412.

(10) Wirmer, J.; Kühn, T.; Schwalbe, H. *Angew. Chem.* **2001**, *113*, 4378−4380.

(11) Dobson, C. M.; Hore, P. J. *Nat. Struct. Biol., NMR supplement* **1998**, *5*, 504−507.

(12) Lyon, C. E.; Suh, E.-S.; Dobson, C. M.; Hore, P. J. *J. Am. Chem. Soc.* **2002**, *124*, 13018−13024.

(13) Lyon, C. E.; Lopez, J. J.; Cho, B.-M.; Hore, P. J. *Mol. Phys.* **2002**, *100*, 1261−1269.

(14) Hore, P. J.; Winder, S. L.; Roberts, C. H.; Dobson, C. M. *J. Am. Chem. Soc.* **1997**, *119*, 5049−5050.

(15) Hore, P. J.; Kaptein, R. Photochemically induced dynamic nuclear polarization (photo-CIDNP) of biological molecules using continuous wave and time-resolved methods. In *NMR Spectroscopy*: *New Methods and Applications*; Levy, G. C., Ed.; ACS Symposium Series 191; American Chemical Society: Washington, 1982; pp 285−318.

(16) Miller, R. J.; Closs, G. L. *Rev. Sci. Instrum.* **1981**, *52*, 1876−1885.

(17) Tsentalovich, Y. P.; Morozova, O. B.; Yurkovskaya, A. V.; Hore, P. J. *J. Phys. Chem. A* **1999**, *103*, 5362−5368.

(18) Tsentalovich, Y. P.; Morozova, O. B.; Yurkovskaya, A. V.; Hore, P. J.; Sagdeev, R. Z. *J. Phys. Chem. A* **2000**, *104*, 6912−6916.

(19) Tsentalovich, Y. P.; Morozova, O. B. *J. Photochem. Photobiol., A: Chem.* **2000**, *30*, 33−40.

(20) Morozova, O. B.; Yurkovskaya, A. V.; Tsentalovich, Y. P.; Forbes, M. D. E.; Sagdeev, R. Z. *J. Phys. Chem. B* **2002**, *106*, 1455−1460.

(21) Morozova, O. B.; Yurkovskaya, A. V.; Vieth, H.-M.; Sagdeev, R. Z. *J. Pys. Chem. B* **2003**, *107*, 1088−1096.

(22) Morozova, O. B.; Yurkovskaya, A. V.; Tsentalovich, Y. P.; Forbes, M. D. E.; Hore, P. J.; Sagdeev, R. Z. *Mol. Phys.* **2002**, *100*, 1187−1195.

(23) Permyakov, E. A.; Berliner, L. J. *FEBS Lett.* **2000**, *473*, 267−274.

(24) Berliner, L. J.; Kaptein, R. *Biochemistry* **1981**, *20*, 799−807.
(25) Lyon, C. E. Photo-CIDNP and Protein Folding. Ph. D. Thesis, Oxford University, 1999.
(26) Hubbard, S. J.; Thornton, J. M. Naccess V2.1.1-Solvent accessible area calculations, http://wolf.bi.umist.ac.uk/naccess, 1996.
(27) Chrysina, E. D.; Brew, K.; Acharya, K. R. *J. Biol. Chem.* **2000**, *275*, 37021−37029.
(28) Ren, J.; Stuart, D. I.; Acharya, K. R. *J. Biol. Chem.* **1993**, *268*, 19292−19298.
(29) Lee, B.; Richards, F. M. *J. Mol. Biol.* **1971**, *55*, 379−400.
(30) Koradi, R.; Billeter, M.; Wüthrich, K. *J. Mol. Graphics* **1996**, *14*, 51−55.
(31) Tsentalovich, Y. P.; Lopez, J. J.; Hore, P. J.; Sagdeev, R. Z. *Spectrochim. Acta, Part A* **2002**, *58*, 2043−2050.
(32) Heelis, P. F.; Parsons, B. J.; Phillips, G. O. *Photochem. Photobiol.* **1978**, *28*, 169−173.
(33) Heelis, P. F.; Parsons, B. J.; Phillips, G. O. *Biochim. Biophys. Acta* **1979**, *587*, 455−462.
(34) Rao, P. S.; Simic, M.; Hayon, E. *J. Phys. Chem.* **1975**, *79*, 1260−1263.
(35) Bradbury, J. H.; Norton, R. S. *Mol. Cell. Biochem.* **1976**, *13*, 113.
(36) Vollenweider, J.-K.; Fischer, H. *Chem. Phys.* **1988**, *124*, 333−345.
(37) Hany, R.; Fischer, H. *Chem. Phys.* **1993**, *172*, 131−146.
(38) den Hollander, J. A. *Chem. Phys.* **1975**, *10*, 167−184.
(39) Miura, T.; Maeda, K.; Arai, T. *J. Phys. Chem. B* **2003**, *107*, 6474−6478.
(40) Wijesinha-Bettoni, R.; Dobson, C. M.; Redfield, C. *J. Mol. Biol.* **2001**, *312*, 261−273.